

Properties of a Composite Material Based on a Copper-Containing Metal-Organic Framework and Graphene Oxide

V. A. Zhinzhilo^a, E. A. Lebedintseva^a, V. N. Naumkina^a, and I. E. Uflyand^{a,*}

^a Southern Federal University, Rostov-on-Don, 344090 Russia

*e-mail: ieuflyand@sfedu.ru

Received May 18, 2021; revised July 13, 2021; accepted August 13, 2021

Abstract—A procedure was developed for *in situ* preparation of a composite material consisting of graphene oxide and a copper-containing metal-organic framework by the reaction between 1,3,5-benzenetricarboxylic acid, graphene oxide, and copper sulfate. The materials obtained were examined by X-ray diffraction, IR spectroscopy, scanning electron microscopy, and energy-dispersive X-ray microanalysis. The composite was used for removing organic dyes Congo Red and Methylene Blue from their aqueous solutions. The samples containing 20% graphene oxide showed the highest adsorption rate. The structure of the composite does not change in the course of the sorption.

Keywords: copper(II) trimesate, graphene oxide, metal-organic framework, composite, organic pollutants, adsorption

DOI: 10.1134/S1070427221080061

Metal-organic frameworks consisting of metal ions or clusters and organic linkers [1, 2] are characterized, on the one hand, by a three-dimensional porous crystal structure, diversity of framework structures and topologies, large pore volume, and large amount of active sites and, on the other hand, by good thermal stability and by useful magnetic, optical, and other properties [3, 4].

However, wide use of these materials is restricted by such drawbacks as poor moisture resistance, structural degradation under the action of high pressure and temperature, insufficient light stability, and low levels of electrical conductivity and mechanical strength [5, 6]. To expand applications of metal-organic frameworks, it seems promising to develop their composites with other materials, so as to obtain polyfunctional materials with improved properties [7, 8]. Such composites exhibit enhanced stability, increased electrical conductivity, high strength, chemical and thermal stability, water resistance, and valuable mechanical properties [9, 10]. In addition, higher surface area and porosity are important

advantages of the composites over unmodified metal-organic frameworks [11, 12].

Because the conditions for preparing the composites can significantly affect the nature of the interaction between the metal-organic frameworks and graphene oxide and hence the properties of the composite, various strategies were developed for preparing such materials. The *in situ* synthesis procedure consists in preparation of metal-organic frameworks in the presence of graphene oxide. An indubitable advantage of the synthesis of composites consisting of metal-organic frameworks and graphene oxide using this approach is that the synthesis is simple and rapid [13, 14]. Oxidized functional groups of graphene oxide act as growth sites of metal-organic framework structures. Introduction of graphene oxide into metal-organic frameworks increases the surface area and porosity and improves the morphology and sorption characteristics of the materials.

This study was aimed at preparing a composite based on copper trimesate and graphene oxide by the in

situ procedure and at determining the properties of the material obtained.

EXPERIMENTAL

We used commercially available chemicals: 1,3,5-benzenetricarboxylic acid (98%, Acros Organics, catalog no. 105350500), NaOH (technical grade, Kaustik, Russia), and CuSO₄·5H₂O (99%+, Acros Organics, catalog no. 197720050). As solvents we used ethanol, methanol, ethyl acetate, and dichloromethane (all chemically pure grade, Reakhim, Russia). All the chemicals were used without preliminary treatment and purification.

As starting material we used S-1 flaky graphite (technical grade, Lenreaktiv, Russia) without additional purification. The graphite particle size was 125–1000 µm (mean size 200 µm). Graphene oxide was prepared by the Hummers method [15] in accordance with the previously developed protocol [16].

The composite was prepared in two steps. In the first step, we prepared a soluble form of 1,3,5-benzenetricarboxylic acid (sodium salt). To an aqueous solution containing 0.09 mol of sodium hydroxide in 50 mL of water, we added with heating to 80°C 0.03 mol of the acid. The pH was maintained in the range 5.5–6.0. In the second step, to the sodium trimesate solution obtained we added an aqueous suspension of graphene oxide and an aqueous solution of 0.03 mol of copper sulfate. The precipitate formed was filtered off, dried in air, and treated in succession with alcohol, dry ethyl acetate, and dichloromethane, with keeping in each solvent for 8 h. After that, the precipitate was separated by centrifugation, washed with dry dichloromethane, and dried for 10 h in a dynamic vacuum at 120°C. Graphene oxide was introduced into the composite in amounts of 5, 10, and 20% relative to the calculated copper trimesate weight. After the synthesis, the material was thoroughly dried with the replacement of water in the composite by dichloromethane, followed by the solvent removal.

X-ray diffraction (XRD) analysis was performed with a Phywe XR 4.0 device (Phywe, Cu_{Kα}, $\lambda = 0.15418$ nm, scanning rate 2 deg min⁻¹, step 0.02°). The Fourier transform IR (FTIR) spectra were taken with a Perkin Elmer Spectrum 100 FTIR spectrometer (Perkin Elmer) from KBr pellets using Softspectra software for the data analysis (Shelton, CT). Scanning electron microscopic

(SEM) images were taken with a ZEISS Crossbeam 340 device (Carl Zeiss) at an accelerating voltage of 3 kV. Secondary electrons were detected with an Everhart-Thornley detector (SE2). The magnification was varied from 1.92 to 50 000. The distribution of chemical elements on the sample surface was determined by energy-dispersive X-ray (EDX) microanalysis using an Oxford X-max 80 microanalyzer (Oxford Instruments) with the electron probe energy of ≤10 keV.

As adsorbates we chose Methylene Blue and Congo Red dyes (Sigma-Aldrich, catalog nos. 556416 and B24310.14). The concentration of their stock aqueous solution was 200 mg L⁻¹. Working solutions were prepared by dilution of the stock solution with distilled water (Liston A 1104 distiller) to the required working concentrations.

The adsorption was studied in batch experiments [17]. A dye solution (200 mL) was placed in a beaker and thermostated at 283, 293, and 308 K on a magnetic stirrer. The rotation rate was chosen so as to ensure efficient stirring and, on the other hand, to avoid the air drawing into the liquid phase. The sorbent was added when the preset temperature was reached. At 15-min intervals, a 10-mL sample of the sorbent suspension in the dye solution was taken and centrifuged; the residual dye concentration in the filtrate was determined with a Cary 50 UV-visible spectrophotometer (Varian) at $\lambda_{\text{max}} = 492$ (Congo Red) and 664 nm (Methylene Blue) [18]. In all the cases, high coefficients of determination R^2 (0.837–0.991) were obtained.

The adsorption value was calculated by the following equations:

$$q_t = (c_0 - c_t)V / m, \quad (1)$$

$$q_e = (c_0 - c_e)V / m, \quad (2)$$

where q_t and q_e are the amounts (mg g⁻¹) of the dye adsorbed at time t and at equilibrium, respectively; c_0 , c_t , and c_e are dye concentrations in the solution (mg L⁻¹) at the initial moment, at time t , and at equilibrium, respectively; m (g) is the sorbent amount; and V (L) is the dye solution volume.

The degree of adsorption A (%) (degree of adsorbate removal) was calculated by the formula

$$A = (c_0 - c_e)/c_0 \times 100. \quad (3)$$

The Gibbs free energy (ΔG) and the standard enthalpy (ΔH) and entropy (ΔS) were calculated from

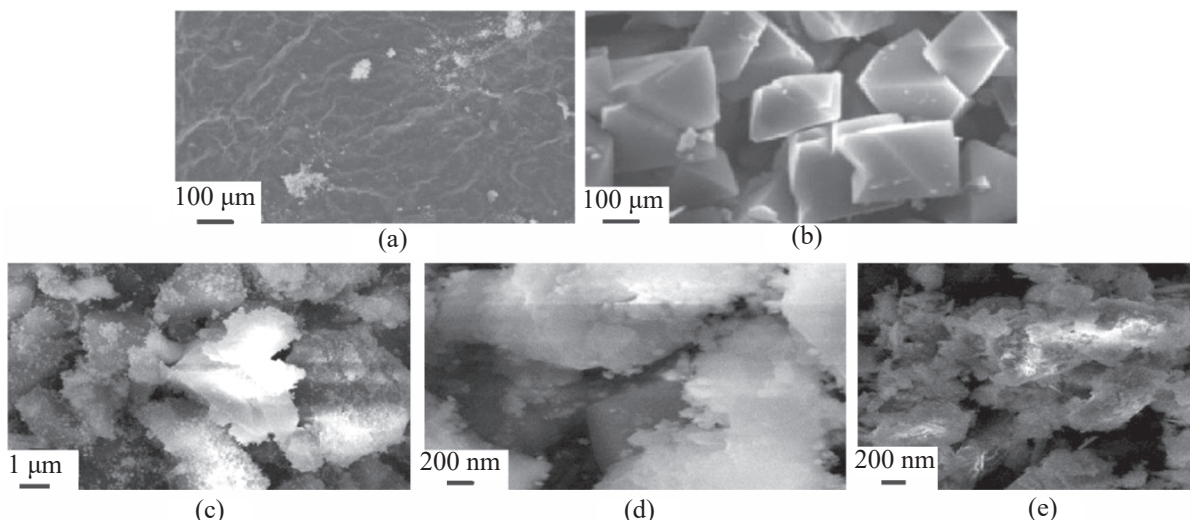


Fig. 1. SEM images of the composite and starting components. (a) Graphene oxide, (b) copper trimesate, and (c–e) composites of copper trimesate with 5, 10, and 20% graphene oxide, respectively.

the adsorption isotherms at different temperatures. The thermodynamic characteristics can be calculated analytically using the equations

$$\Delta H = \frac{\ln \frac{K_1}{K_2} RT_1 T_2}{T_2 - T_1}, \quad (4)$$

$$\Delta G = \Delta H - T \Delta S, \quad (5)$$

where K_1 and K_2 are the adsorption equilibrium constants at temperatures T_1 and T_2 , respectively, and R is the universal gas constant.

RESULTS AND DISCUSSION

The content of elements in the graphene oxide sample obtained, determined by EDX analysis and combustion, was as follows (%): 66.5 ± 0.1 (carbon), 31.8 (oxygen), and 1.72 (hydrogen).

Graphene oxide particles are aggregates in the form of stacks of long nanosheets less than 100 nm thick; defects and folds can be seen on their edges (Fig. 1a).

The synthesized graphene oxide was identified by XRD (Fig. 2a). The diffraction pattern of the sample has a well-defined peak in the region of 11.4° , corresponding to graphene oxide, with the corresponding large d -spacing (0.998 nm). This pattern reasonably agrees with the data from [19, 20]. According to [21], strongly oxidized graphene oxide is characterized by the d -spacing of approximately 1 nm; thus, the formation

of strongly oxidized graphene oxide in our study can be assumed. The diffraction pattern of the graphene oxide obtained has an ill-defined peak at $\sim 25.1^\circ$, suggesting the presence of a small amount of unoxidized graphite. These particles have a more ordered structure and are centers of orientation of distorted graphene oxide (minimizing its potential energy) [22, 23]. In the UV-visible absorption spectrum of graphene oxide from aqueous suspension, there is a peak in the region of 235 nm, corresponding to $\pi-\pi^*$ transitions of the sp^2 C–C bonds (Fig. 2b).

The IR spectrum contains a peak in the region of 3400 cm^{-1} , assignable to stretching vibrations of hydroxy groups of adsorbed water, and a strong band in the region of 1730 cm^{-1} , corresponding to vibrations of carboxyl groups and epoxy carbon atoms. The absorption band in the region of 1640 cm^{-1} is assigned to bending vibrations of hydroxy groups. Strong absorption bands at 1222 and 1050 cm^{-1} can also characterize the formation of epoxy groups. These data well agree with the results of studying laboratory and commercial samples of graphene oxide [19, 20].

The composites have a unique layered structure in which the graphene oxide blocks are separated by metal-organic frameworks. A strong band at 3400 cm^{-1} in the IR spectrum suggests the presence of adsorbed water.

The composite does not form such dense structure as the initial coordination polymer does (Fig. 1b) but has a layered structure irrespective of the amount of

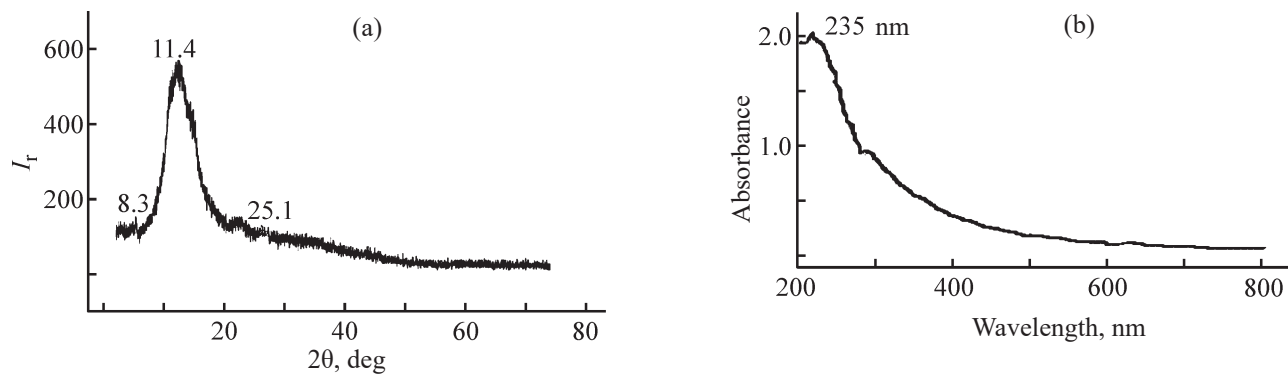


Fig. 2. (a) Diffraction pattern and (b) UV-visible absorption spectrum of a graphene oxide sample.

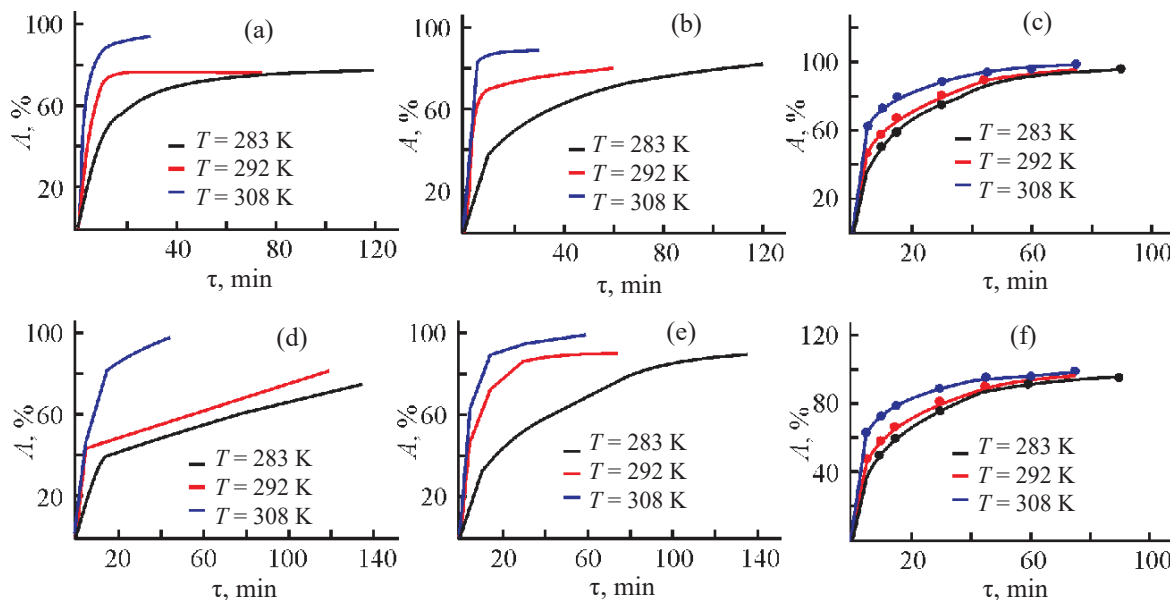


Fig. 3. (Color online) Degree of adsorption of (a–c) Congo Red and (d–f) Methylene Blue onto composites containing copper trimesate and (a, d) 5, (b, e) 10, and (c, f) 20% graphene oxide as a function of time at different temperatures.

the introduced graphene oxide (Figs. 1c–1e). Graphene oxide sheets are directly adjacent to copper trimesate crystals, forming a common system. The diffraction patterns of the composites have similar shape, which does not depend on the graphene oxide content, and coincide with the previously published data [24].

We examined the ability of the composite containing 5, 10, and 20% graphene oxide to adsorb organic dyes from their aqueous solutions. As investigation objects we chose Methylene Blue (cationic dye) and Congo Red (anionic dye), which are technogenic pollutants [25]. The adsorption of the dyes onto the composite rapidly increases in the initial period of contact and then decelerates (Fig. 3). Rapid diffusion to the external surface is accompanied by the diffusion into the matrix

pores at relatively high rate, so that the equilibrium is attained quickly. The adsorption of Congo Red onto the composite is higher than that of Methylene Blue.

The composite exhibits satisfactory sorption activity with respect to both dyes, but the process rate strongly depends on the weight fraction of the introduced graphene oxide. The adsorption rate is the highest for the samples containing 20% graphene oxide. The adsorption onto the composite containing 5 and 10% graphene oxide depends on temperature; hence, it was interesting to study the thermodynamics of this process.

The negative values of the Gibbs free energy, indicating that the adsorption is spontaneous, are determined by the positive entropy of adsorption and

Table 1. Thermodynamic functions of the adsorption of Congo Red and Methylene Blue onto a composite of graphene oxide and a metal-organic framework

Dye	T, K	Graphene oxide content of the composite 5%			Graphene oxide content of the composite 10%			Graphene oxide content of the composite 20%		
		ΔH , kJ mol ⁻¹	ΔG , kJ mol ⁻¹	ΔS , J mol ⁻¹ K ⁻¹	ΔH , kJ mol ⁻¹	ΔG , kJ mol ⁻¹	ΔS , J mol ⁻¹ K ⁻¹	ΔH , kJ mol ⁻¹	ΔG , kJ mol ⁻¹	ΔS , J mol ⁻¹ K ⁻¹
Congo Red	283	-15.6	-75.5	211.6	-20.4	-89.5	244.2	-25.3	-102.4	272.4
	291	-17.2	-82.3	220.7	-23.2	-96.7	252.6	-29.6	-115.2	291.1
	308	-22.3	-97.2	243.2	-26.6	-107.4	262.3	-34.3	-128.4	305.0
Methylene Blue	283	-10.3	-86.7	270.0	-12.4	-98.2	303.2	-17.5	-112.6	336.0
	291	-22.4	-92.4	240.5	-29.3	-109.7	276.3	-23.5	-119.4	329.5
	308	-66.2	-101.4	114.3	-74.6	-107.4	106.5	-29.2	-120.3	295.8

negative enthalpy of adsorption (exothermic process, Table 1). Lower adsorption of cationic Methylene Blue compared to anionic Congo Red may be caused by the competing effect that water occupying open metal sites in the architecture of the composite exerts on the adsorption of Lewis base $[-N(CH_3)_2]$ groups of Methylene Blue. The adsorption of the dyes onto the composites containing 5 and 10% graphene oxide strongly depends on temperature, whereas for the composite containing 20% graphene oxide such dependence is less pronounced. The Gibbs free energy decreases with increasing temperature, which means that an increase in the temperature favors spontaneous occurrence of the adsorption.

The experimentally found values of ΔG can also be used for determining the kind of adsorption. At ΔG from 0 to -20 kJ mol⁻¹, physical adsorption is more probable, whereas chemisorption is characterized by ΔG from -80 to -400 kJ mol⁻¹. For Methylene Blue, the chemisorption is more pronounced because of the fact that graphene oxide containing sufficient amount of carboxyl groups chemically binds Methylene Blue, whereas the physical sorption of the dye is limited [26].

The products of dye adsorption onto the composite were examined by XRD. No changes in the crystal structure of the composite upon sorption were observed (Fig. 4).

CONCLUSION

The developed one-step method for *in situ* synthesis of composites based on a copper-containing metal-organic

framework and graphene oxide is cost-saving and can be used for large-scale production. The composites have a unique layered structure in which graphene oxide blocks are separated by metal-organic frameworks. A study of the ability of the composites to adsorb organic dyes (Congo Red and Methylene Blue) has shown that the adsorption largely depends on the graphene oxide content of the composites. The adsorption does not noticeably affect the crystal structure of the starting composite. The composite material obtained can be demanded as a sorbent for solid-phase extraction of organic dyes.

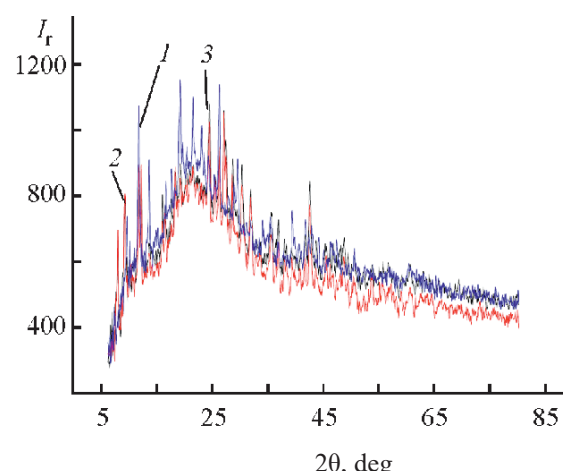


Fig. 4. Diffraction patterns (1) of the initial composite containing copper trimesate and 10% graphene oxide and of the composite after contact with solutions of (2) Congo Red and (3) Methylene Blue.

CONFLICT OF INTEREST

The authors declare that they have no conflict of interest.

AUTHOR CONTRIBUTION

V.A. Zhinzhilo and I.E. Uflyand: synthesis of the composite and study of its composition and structure; E.A. Lebedintseva and V.N. Naumkina: study of the dye adsorption onto the synthesized composite.

REFERENCES

1. Dzhardimalieva, G.I. and Uflyand, I.E., *Chemistry of Polymeric Metal Chelates*, Cham: Springer, 2018, pp. 633–759.
2. Butova, V.V., Soldatov, M.A., Guda, A.A., Lomachenko, K.A., and Lamberti, C., *Russ. Chem. Rev.*, 2016, vol. 85, no. 3, pp. 280–307.
<https://doi.org/10.1070/RCR4554>
3. Tsivadze, A.Yu., Aksyutin, O.E., Ishkov, A.G., Knyazeva, M.K., Solovtsova, O.V., Men'shchikov, I.E., Fomkin, A.A., Shkolin, A.V., Khozina, E.V., and Grachev, V.A., *Russ. Chem. Rev.*, 2019, vol. 88, no. 9, pp. 925–978.
<https://doi.org/10.1070/RCR4873>
4. Ahamed, M.N., Khan, M.S., Shahid, M., and Ahmad, M., *Dalton Trans.*, 2020, vol. 49, no. 41, pp. 14690–14705.
<https://doi.org/10.1039/D0DT02949A>
5. Veltlitsyna-Novikova, K.S., Butova, V.V., Pankin, I.A., Shapovalov, V.V., and Soldatov, A.V., *J. Synch. Investig.*, 2019, vol. 13, no. 5, pp. 787–792.
<https://doi.org/10.1134/S1027451019050173>
6. Yuan, S., Feng, L., Wang, K., Pang, J., Bosch, M., Lollar, C., Sun, Y., Qin, J., Yang, X., Zhang, P., Wang, Q., Zou, L., Zhang, Y., Zhang, L., Fang, Y., Li, J., and Zhou, H.C., *Adv. Mater.*, 2018, vol. 30, no. 37, ID 1704303. <https://doi.org/10.1002/adma.201704303>
7. Chen, L., Zhang, X., Cheng, X., Xie, Z., Kuang, Q., and Zheng, L., *Nanoscale Adv.*, 2020, vol. 2, no. 7, pp. 2628–2647.
<https://doi.org/10.1039/D0NA00184H>
8. Al Amery, N., Abid, H.R., Al-Saadi, S., Wang, S., and Liu, S., *Mater. Today Chem.*, 2020, vol. 17, ID 100343.
<https://doi.org/10.1016/j.mtchem.2020.100343>
9. Zheng, Y., Zheng, S., Xue, H., and Pang, H., *Adv. Funct. Mater.*, 2018, vol. 28, no. 47, ID 1804950.
<https://doi.org/10.1002/adfm.201804950>
10. Jayaramulu, K., Horn, M., Schneemann, A., Saini, H., Bakandritsos, A., Ranc, V., Petr, M., Stavila, V., Narayana, C., Scheibe, B., Kment, Š., Otyepka, M., Motta, N., Dubal, D., Zbořil, R., and Fischer, R.A., *Adv. Mater.*, 2021, vol. 33, no. 4, ID 2004560.
<https://doi.org/10.1002/adma.202004560>
11. Arslanov, V.V., Kalinina, M.A., Ermakova, E.V., Raitman, O.A., Grachev, V.A., Tsivadze, A.Y., Gorbunova, Y.G., Aksyutin, O.E., and Ishkov, A.G., *Russ. Chem. Rev.*, 2019, vol. 88, no. 8, pp. 775–799.
<https://doi.org/10.1070/RCR4878>
12. Todaro, M., Buscarino, G., Sciortino, L., Alessi, A., Messina, F., Taddei, M., Ranocchiari, M., Cannas, M., and Gelardi, F.M., *J. Phys. Chem. C*, 2016, vol. 120, no. 23, pp. 12879–12889.
<https://doi.org/10.1021/acs.jpcc.6b03237>
13. Liu, N., Huang, W., Zhang, X., Tang, L., Wang, L., Wang, Y., and Wu, M., *Appl. Catal. B*, 2018, vol. 221, pp. 119–128.
<https://doi.org/10.1016/j.apcatb.2017.09.020>
14. Hu, Y., Wei, J., Liang, Y., Zhang, H., Zhang, X., Shen, W., and Wang, H., *Angew. Chem. Int. Ed.*, 2016, vol. 55, no. 6, pp. 2048–2052.
<https://doi.org/10.1002/anie.201509213>
15. Hummers, W.S., Jr. and Offeman, R.E., *J. Am. Chem. Soc.*, 1958, vol. 80, no. 6, p. 1339.
<https://doi.org/10.1021/ja01539a017>
16. Novikova, A.A., Burlakova, V.E., Varavka, V.N., Uflyand, I.E., Drogan, E.G., and Irkha, V.A., *J. Mol. Liq.*, 2019, vol. 284, pp. 1–11.
<https://doi.org/10.1016/j.molliq.2019.03.111>
17. Neff, H., Laborde, H.M., and Lima, A.M.N., *Sci. Rep.*, 2016, vol. 6, ID 36232.
<https://doi.org/10.1038/srep36232>
18. Dzhardimalieva, G., Baimuratova, R., Knerelman, E., Davydova, G., Kudaibergenov, S., Kharissova, O., Zhinzhilo, V., and Uflyand, I., *Polymers*, 2020, vol. 12, no. 5, ID 1024.
<https://doi.org/10.3390/polym12051024>
19. Lian, P., Zhu, X., Liang, S., Li, Z., Yang, W., and Wang, H., *Electrochim. Acta*, 2010, vol. 55, no. 12, pp. 3909–3914.
<https://doi.org/10.1016/j.electacta.2010.02.025>
20. Manoratne, C.H., Rosa, S.R.D., and Kottegoda, I.R.M., *Mater. Sci. Res. India*, 2017, vol. 14, no. 1, pp. 19–30.
<http://dx.doi.org/10.13005/msri/140104>
21. Buchsteiner, A., Lerf, A., and Pieper, J., *J. Phys. Chem. B*,

- 2006, vol. 110, no. 45, pp. 22328–22338.
<https://doi.org/10.1021/jp0641132>
22. Kim, S., Zhou, S., Hu, Y., Acik, M., Chabal, Y.J., Berger, C., de Heer, W., Bongiorno, A., and Riedo, E., *Nature Mater.*, 2012, vol. 11, pp. 544–549.
<https://doi.org/10.1038/nmat3316>
23. Gupta, B., Kumar, N., Titovich, K.A., Kolesnikov, V.I., Sidashov, A.V., and Dash, S., *Surf. Interfaces*, 2017, vol. 7, pp. 6–13.
<https://doi.org/10.1016/j.surfin.2017.02.005>
24. Domán, A., Klébert, S., Madarász, J., Sáfrán, G., Wang, Y., and László, K., *Nanomaterials*, 2020, vol. 10, no. 6, ID 1182.
<https://doi.org/10.3390/nano10061182>
25. Lafi, R., Montasser, I., and Hafiane, A., *Adsorption Sci. Technol.*, 2019, vol. 37, nos. 1–2, pp. 160–181.
<https://doi.org/10.1177/0263617418819227>
26. Nanthamathee, C. and Dechatiwongse, P., *Mater. Chem. Phys.*, 2021, vol. 258, ID 123924.
<https://doi.org/10.1016/j.matchemphys.2020.123924>